Hindawi
Journal of Nanomaterials
Volume 2020, Article ID 4297937, 10 pages
https://doi.org/10.1155/2020/4297937

Research Article

A Unique Protein Self-Assembling Nanoparticle with Significant Advantages in Vaccine Development and Production

Daniel C. Carter,[1,2] **Brenda Wright**,[1] **W. Gray Jerome**,[3] **John P. Rose**,[4] **and Ellen Wilson**[1]

[1]*Albumin Therapeutics, LLC, 895 Martin Road SW, Huntsville, AL, USA*
[2]*New Century Pharmaceuticals, Inc., 895 Martin Road SW, Huntsville, USA*
[3]*Vanderbilt University, Department of Pathology, Microbiology and Immunology, Vanderbilt University School of Medicine, U2206 MCN, 1161 21st Ave., South, Nashville, TN, USA*
[4]*University of Georgia, Department of Biochemistry and Molecular Biology, 120 Green St., Athens, GA, USA*

Correspondence should be addressed to Daniel C. Carter; dcarter@albuminbio.com

Received 24 May 2019; Revised 8 October 2019; Accepted 23 October 2019; Published 4 January 2020

Academic Editor: Laura Martinez Maestro

Nanoparticles are playing an increasingly powerful role in vaccine development. Here, we report the repurposing of nonstructural proteins 10 and 11 (hereafter NSP10) from the replicase polyprotein 1a (pp1a) of the human SARS coronavirus (severe acute respiratory syndrome) as a novel self-assembling platform for bioengineered nanoparticles for a variety of applications including vaccines. NSP10 represents a 152 amino acid, 17 kD zinc finger transcription/regulatory protein which self-assembles to form a spherical 84 Å diameter nanoparticle with dodecahedral trigonal 32 point symmetry. As a self-assembling nanoparticle, NSP10 possesses numerous advantages in vaccine development and antigen display, including the unusual particle surface disposition of both the N- and C-termini. Each set of N- or C-termini is spatially disposed in a tetrahedral arrangement and positioned at optimal distances from the 3-fold axes (8-10 Å) to nucleate and stabilize the correct folding of complex helical or fibrous trimeric receptors, such as those responsible for viral tropism and cell infection. An application example in the exploratory development of a therapeutic vaccine for idiopathic pulmonary fibrosis (IPF), including preliminary analysis and immunogenic properties, is presented. The use of this system could accelerate the discovery and development of vaccines for a number of human, livestock, and veterinary applications.

1. Introduction

Nanoparticle-based materials are an area of extensive research, largely due to the changes in physical properties of materials as they approach the 10 nm size. Their compositions are varied and include a full spectrum of pure or composite materials which can range from metals, such as gold or silver to biological-based particles, which include viruses or engineered virus-like particles (VLP).

A particularly powerful application of VLPs is to create fusion proteins which display microbial or viral antigens on the nanoparticle surface. It has been shown that VLP antigen fusions can dramatically enhance the magnitude (10- to 100-fold) and quality of the immune response [1–4]. VLPs can in some cases aid in the formation and display of viral receptor stems with native oligomeric structure, an essential property of effective vaccines which elicit potent and broadly neutralizing antibodies. These viral receptors are considered among the most important immunization targets in vaccine development since they are often key in eliciting neutralizing antibodies that prevent viral infection by blocking the viral receptor interaction or preventing the conformational transition required for subsequent membrane fusion. Viruses employ such receptors either directly on capsid surface or extending from the surface in helical or fibrous trimeric stems. Important examples of viruses that utilize trimeric stem-based receptor assemblies include influenza virus, human immunodeficiency virus (HIV), Ebola virus, and viruses of the coronavirus, reovirus, and adenovirus families. However, the engineering and display of trimeric receptors on VLPs can be limited by the sequence polarity required for the protein fusions. This is because the protein sequence

polarity of the receptor stem as it extends from the virus or nanoparticle surface dictates the requirement for C- or N-terminus VLP fusion. For example, the viral receptor stems of influenza virus, HIV, Ebola virus, and the coronaviruses all require fusion through the N-terminus of the VLP, while those of the reovirus and adenovirus families, the C-terminus. Most importantly, a critical requirement for engineering VLP display of these receptors is a trimeric disposed arrangement of the N- or C-termini on the VLP surface with appropriate radial spacing from 3-fold symmetry elements.

One highly successful example of a nonviral-based VLP self-assembling nanoparticle system is ferritin [1]. Ferritin is an iron storage protein found in all living systems which self-assembles into a 24-mer capsid having 432 cubic point group symmetry with a diameter of 12 nm [5]. In the case of ferritin, the N-termini of each of the 24 monomeric units terminate on the capsid surface, making it possible to engineer fusion proteins to display antigens and create vaccines. It has been exploited for the exploration of a number of vaccines [2–4, 6] and notably promoted by the National Institutes of Health (NIH) as the path to the universal flu vaccine [7]. Most recently, ferritin has been used to delineate immune-mediated glycosylation-dependent recognition pathways which further emphasizes the advantages of nanoparticle-based vaccines and may have broad implications in future vaccine design [6].

Here, we report the repurposing of coronavirus NSP10-type proteins as bioengineered self-assembling nanoparticles for a variety of applications including vaccine development [8]. Structurally, NSP10 is a 17 kD protein which self-assembles into a spherical dodecahedral nanoparticle with trigonal 32 point symmetry (Figure 1) having an outer diameter of 84 Å and an inner hollow core of 36 Å diameter (Su et al., 2006; PDB identifier: 2G9T, UniProt sequence identifier P0C6U8). NSP10s represent a family of proteins that have only been identified in the coronavirus genus (groups I, II, and III), share no sequence homology with any other known proteins, and are highly conserved within the coronavirus genus implying the overall importance in the viral transcription machinery and a common oligomeric assembly. They are components of the replicase polyprotein 1a (pp1a) of the human SARS coronavirus (severe acute respiratory syndrome) which contains 11 proteins (nonstructural proteins, NSP1-11) produced by viral specific cleavage upon productive infection. The polyprotein pp1a sequence encompassing residues 4231 to 4382 represents a 152 amino acid zinc finger transcription/regulatory protein which is comprised of both nonstructural proteins 10 and 11 (NSP10 and NSP11). Hereafter, as in Su et al (2006), we refer to this 152 amino acid protein for convenience as NSP10, as well as reflect a new primary sequence numbering of 1 to 152.

The folding topology of NSP10 is a mixed alpha helical and beta sheet structure which can be further described as having two pseudo-subdomains, a small alpha helical bundle, we denote as subdomain I (residues and helical regions 1-39; 70-91; 104-115) and a small beta sheet domain, we denote as subdomain II (residues 40–70; 90-105). The helical subdomains I self-associate to form a trimer interaction at the four

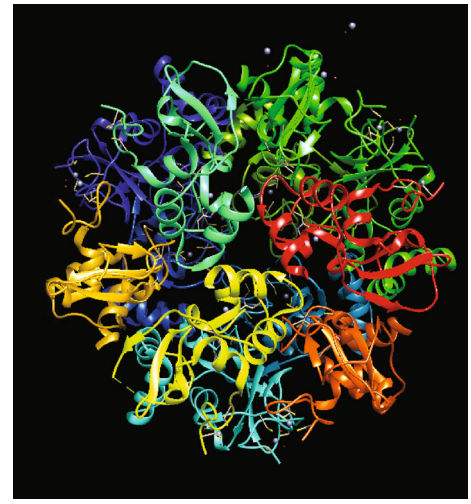

Figure 1: Structure of the NSP10 dodecamer NSP10 dodecahedron as viewed down one of the threefold axes showing the close association of the three N-terminal helices of subdomain I. Each monomeric protein, twelve in total, is shown in a different color. An important consequence of the NSP10 particle point symmetry (point group 32) is that each N-terminal threefold set has a corresponding C-terminal set which is collinear on the same 3-fold axis, but located on the directly opposite capsid surface. The depicted NSP10 oligomer represents residues 9 to 129. The illustration was created using coordinates from the Protein Data Bank (PDB): 2G9T [9] and the program Chimera.

capsid N-terminal threefold axes and subdomains II self-associate as trimeric units on the four C-terminal threefold axes. One zinc binding site was observed by crystallography at the interface between the two subdomains in addition to three other zinc sites located within subdomain II near the C-terminus [9]. The essential capsid encompasses residues 9-129 and hereafter it is this truncated sequence that constitutes the NSP10 used in the subsequent fusion protein design, *vida infra*.

The particle symmetry can be conceptualized as a trigonal pyramid (tetrahedron) where there are two sets of tetrahedral disposed threefold axes: (1) those located at each pyramid apex and (2) those located at the center of each lateral face (Figure 2). This provides the capability to create surface displayed protein fusions at either terminus. In addition to the monomeric display of protein and peptide antigens, each set of N- or C-termini is positioned radially at optimal distances from the 3-fold axes (8-10 Å) to nucleate and stabilize the correct folding of complex helical or fibrous trimeric receptors, such as those responsible for viral tropism and cell infection. This feature is an important and rare feature of this protein which is of further potential advantage since there is compelling evidence that a trimeric scaffold is essential to nucleate and stabilize the proper native structural assembly of fibrous trimeric stems, and possibly other important trimeric assemblies [10, 11].

The capsid allows for a total of 24 displays of peptide or protein fusions on the particle surface with 12 from the N-terminus and 12 from the C-terminus. In the case of trimeric stem displays, such as through a hemagglutinin

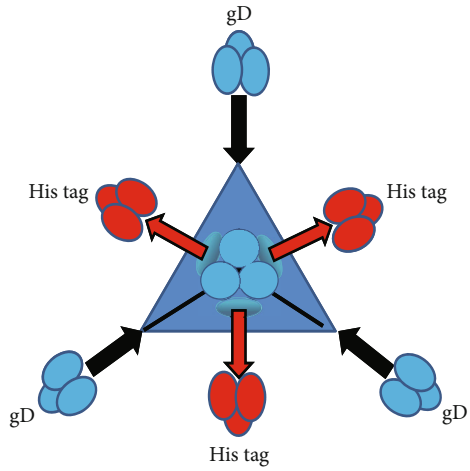

Figure 2: Conceptualized NSP10 particle symmetry The symmetry and fusion polarity of NSP10 as depicted by a tetrahedron. The example shown is illustrative of the NSP10 HVS gD nanoparticle discussed in the following sections where gD shown in blue and His-tag, shown in red, are fused through N-terminus and C-terminus, respectively. Here, the threefold sets of the NSP10 N-termini are shown at each pyramid apex with the corresponding C-termini fused His-tags shown in red emanating from each of the threefold axes centered on each lateral face. Arrows denote the direction of the polypeptide chain from the N- to the C-termini.

fusion (N-terminal fusion), this creates a tetrahedral display as shown in Figure 3(a). The C-termini, shown as red patches on the particle surface in Figure 3(a), allow for the potential of multivalent vaccines, such as a complimentary tetrahedral stem display (Figure 3(b)). Thus, in principle, any number of combinations can be explored. For example, there can be combinations of stems and monomeric antigen displays at the opposite terminus or one set can incorporate affinity tags for isolation and purification. In DNA vaccine applications, polycistronic expression can be employed where a viral stem, such as hemagglutinin, can be held constant while additional important antigens/proteins are varied at the C-terminus creating a nanoparticle displaying a homogeneous hemagglutinin and a mixture of other important antigens. Clearly, the useful variations which can be explored are manifold.

Although, like ferritin, the NSP10 family of proteins can have many other nanomaterial applications, we limit our discussions to applications in antigen presentation and related therapeutic or vaccine development, and provide an illustrative example in the design of a vaccine for *Herpesvirus saimiri*, (HVS) implicated in IPF [12]. HVS is a γ_2-herpesvirus or rhadinovirus related to the human Kaposi's sarcoma-associated herpesvirus [13]. In its natural host, the squirrel monkey (*Saimiri sciureus*), it does not cause disease and most animals are asymptomatic [13]. However, in new world monkeys and other more dissimilar animals including poultry, it contributes to disease with high morbidity and mortality [13, 14]. Although there is no general consensus on the etiological agent for IPF, the virus theory is compelling for many reasons including the evidence of the role of gamma herpesviruses in the induction of progressive IPF-like diseases in horses and other mammals [14, 15] and observations of the positive effects of administered antivirals in animal model systems of IPF [16].

In humans, IPF is a degenerative lung disease characterized by invasive myofibroblast which remodel and destroy lung epithelial tissue and function [17]. The disease is usually diagnosed later in life as the symptoms become apparent with the majority of the patients in their 50s and 60s. IPF affects approximately 200,000 individuals in the United States and is typically fatal within 3 to 5 years of diagnosis [18–21]. Mortality from this disease has been increasing significantly over the past decade and most recent studies estimate an average incidence of 50 per 100,000 in the United States [22]. Whether this increased incidence is related to improved diagnosis, such as through modern noninvasive imaging, remains unclear. Currently, there are two FDA-approved drugs for the treatment of patients with IPF, pirfenidone [20] and nintedanib [21]; both of which can slow the progression of disease, but are not well tolerated by many patients. There is currently no cure for IPF, and new more effective treatments are urgently needed.

For this NSP10 vaccine application, we have chosen to focus on the assumption that HVS is the etiological agent for IPF based on the scientifically compelling work of Folcik et al. (2014). Research towards effective herpesvirus vaccines, such as vaccine candidates for HHS-2 which incorporate appropriate adjuvants combined with viral proteins such as gD and UL40, exhibit promising signs of progress in animals [23]. However, despite continuing advances with vaccines for human herpesviruses and Epstein-Barr virus, progress has thus far been challenging and currently there are no registered vaccines for a herpesvirus. Based on the encouraging progress by others and our goal of creating a nanoparticle-based therapeutic vaccine against HVS versus the more challenging prophylactic vaccine, we chose to focus our initial efforts on establishing a framework for the NSP10 nanoparticle fusion of HVS gD alone. Gamma herpesvirus gD is one of the 4 proteins (gB, gD, and heterodimer gH/gL) involved in the complex fusion mechanism employed by all herpesviruses [24] and as such has been included as a component of vaccine development for herpesviruses, including human herpes virus-2 (HHS-2) [23]. Among the four fusion proteins, gD is the only one absolutely essential for viral infection. In further support of the selection, gD proteins with single point mutations have rendered engineered HHS-1 constructs noninfective [25] and the sera from HHS-positive patients virtually all have neutralizing antibodies to both gD and gB [26]. While there has been early published research exploring a vaccine from killed HVS virus for the prevention of neoplasia induced by HVS in nonhuman primates [27], to our knowledge, the work described here represents the first attempt to make a vaccine as an approach for the treatment of IPF in humans.

2. Results

2.1. Fusion Protein Vector Design and Expression. To examine the expression, nanoparticle assembly, and antigenic properties of NSP10 fusion proteins, we designed NSP10

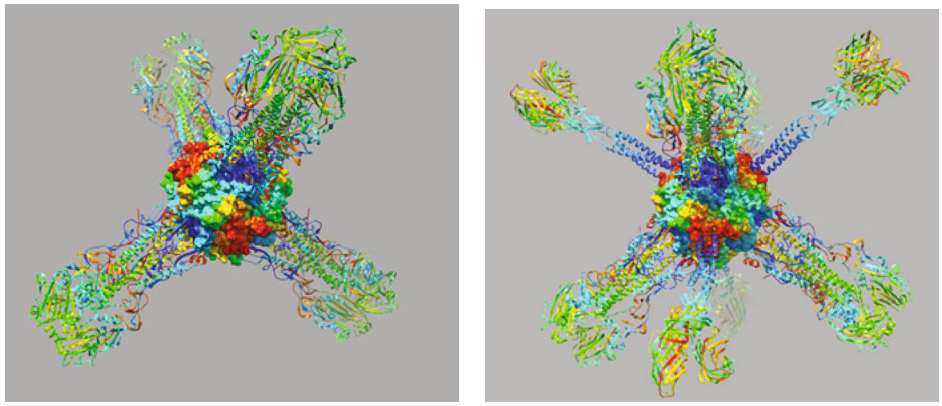

(a) (b)

Figure 3: Hypothetical graphical models of NSP10 fusion proteins. (a) Atomic model illustration depicting NSP10 with a hemagglutinin stem fusion at the N-termini. Note the tetrahedral arrangement provides nonsterically hindered access to the stalk domains. The C-termini are shown as red patches on the capsid surface and provide for the potential of additional protein fusions or affinity tags. (b) Atomic model of a hypothetical NSP10 dual stem display incorporating a hemagglutinin at the N-terminus and a Sigma C reovirus stem at the C-terminus.

fusion protein constructs incorporating a truncated HVS gD for evaluation in two expression vectors: (1) a prokaryotic vector, pET17b for protein expression and purification and (2) a eukaryotic vector, pcDNA3.1(+) for preliminary evaluation of a DNA-based plasmid as a vaccine.

The initial attempts at prokaryotic expression of gD-NSP using pET17b with *E coli* in BL21 cells were unsatisfactory. However, the use of same expression vector in the gram-negative, nonpathogenic marine bacteria, *Vibrio natriegens* (Vmax™) expression system was found to be advantageous providing a good yield of soluble protein and the convenience of simplified cell growth and induction timing. Additionally, at least in this case, the traditional use of DNase enzymes proved unnecessary. Protease inhibitors were intentionally avoided in order to reduce the risks of potential toxicity issues in animals.

Overexpression of the target protein (Vmax™) with the correct estimated MW was indicated by SDS-PAGE (Figures 4(a) and 4(b)) and found to bind efficiently to immobilized metal affinity media. gD-NSP has a calculated monomer MW of 45,958 inclusive of His-tag, resulting in a predicted oligomeric capsid MW of ~551,500 Daltons. To determine whether the self-assembly had occurred, the gD-NSP fusion protein was assessed by Native PAGE (Figures 4(c) and 4(d)). While there is background streaking evident for the native gel, a single uniform band was clearly observed which migrates at a MW greater than horse spleen ferritin capsid (~450,000 Daltons) chosen as a convenient and appropriate MW comparative standard.

TEM analysis of the PBS solution containing the assembled nanoparticles revealed an average particle size of approximately 10.2 nm (Figure 5), as compared with the 8.4 nm diameter of the native NSP10 oligomer determined by X-ray crystallography [9]. Selected particles observed are spherical and provide suggestions of capsid symmetry with visible globular surface components indicative and consistent with the self-assembly of the HVS gD fusion proteins (Figures 5(a) and 5(b)).

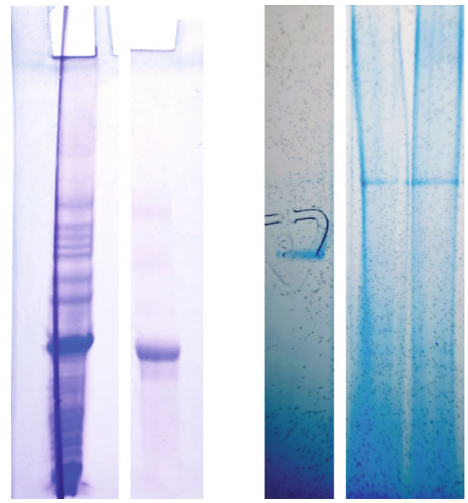

(a) (b) (c) (d) (e)

Figure 4: SDS and Native PAGE of gD-NSP. (a) SDS-PAGE gel showing the overexpression of gD-NSP (MW 45.9 kD) in the crude bacterial lysate. (b) MW reference standard hen's egg ovalbumin, 42.7 kD. Native PAGE electrophoresis gel of (c) horse spleen ferritin MW (450 kD). (d) gD-NSP MW (550 kD) in 50 mM Tris pH 7.5 300 mM NaCl and (e) gD-NSP in PBS, pH 7.4.

2.2. Animal Experiments. Animal studies in rabbits produced notably high titers with both the DNA plasmid-based eukaryotic expression vector in PBS and the isolated and purified gD-NSP protein combined with Adavax™ (a squalene-based adjuvant) after the first and second boosters (Table 1). The DNA vaccine, as a simple IP injection in saline, induced titers of 5,000 after the first booster, but interestingly, a second booster produced a titer of 25,000. The protein vaccine produced titers of 25,000 after the first booster and 625,000 after the second booster. For this study, the vaccines were not tested past a dilution of 1 : 625,000. The utilization of the gD-NSP protein purified from prokaryotic expression to establish the titers and immunogenic response

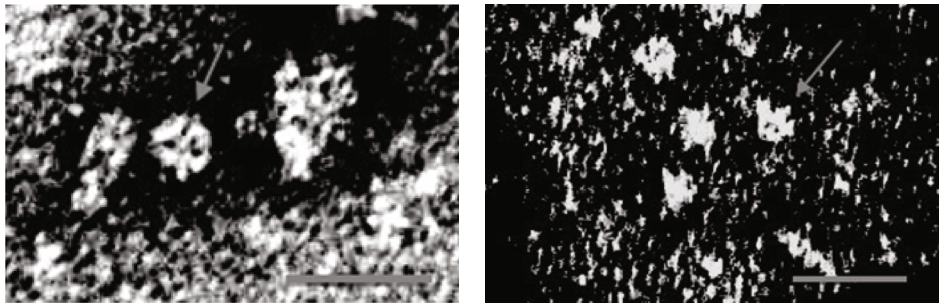

(a) (b)

Figure 5: TEM images (a) and (b) of gD-NSP showing selected spherical nanoparticles with average dimensions of 10.2 nm (102 Å). Arrows indicate example particles. Scale bars shown in the lower left of each image represent 25 nm. Adjustments to the histogram of the original image were made to highlight the particle features without affecting the observed diameter.

Table 1: ELISA titer results. The gD-NSP specific antibodies in animal sera were detected by ELISA. An ELISA was performed on the sera from the animals using the purified gD-NSP and run against negative and positive controls. Antibody was considered present when the optical density (OD) value was greater than or equal to 0.1, normalized against the prebleed. Threshold values were determined as the last dilution giving an OD equal to or greater than 0.1. The titers given below are estimates. Supplemental data are provided in Table S1.

gD-NSP vaccination		Day 0	Day 21	Day 42	Day 63	Day 84	Animal
DNA	Dose	0.5 mg	0.5 mg	None given	0.5 mg	None given	PAS 21917
	Titer	(-)	1,000	5,000	5,000	25,000	PAS 21917
Protein	Dose	1.0 mg	0.1 mg	None given	0.2 mg	None given	PAS 21915
	Titer	(-)	5,000	25,000	5,000	625,000	PAS 21915

of the DNA vaccine shows that highly specific antibodies to the gD-NSP vaccine are elicited by the DNA vaccine. No signs of injection site reactogenicity were observed, and the animals remained healthy throughout the study. The sera from these animals will serve to establish antibodies for Western blot analysis as the project is expanded to include more in-depth studies. Further characterization of the immunology of the vaccine response will be determined in future follow-up studies.

3. Materials and Methods

3.1. HVS gD Fusion Protein Design. Important to the design effort, the atomic structure of a related HHS-1 gD herpesvirus protein has been previously determined by Di Giovine et al. [25] in complex with the nectin-1 receptor, a cell surface adhesion molecule which is the main receptor in epithelial cells and neurons. This structure revealed that HHS-1 gD protein contains a critical large helical peptide section of about 50 amino acids near the C-terminus which was important in receptor binding (Figure 6) [25]. Moreover, altering the flexibility of the 50 amino section of helix has been shown to neutralize the ability of the protein to infect cells. We therefore determined the essential components of the gD HVS design by the alignment of the amino acid sequence with the HHS-1 gD sequence as illustrated in Figure 7. The sequence alignment revealed only 30.4% sequence identity between the two glycoproteins; however, the indications of a common structural topology were easily discerned from the placement of the conserved primary sequence inclusive

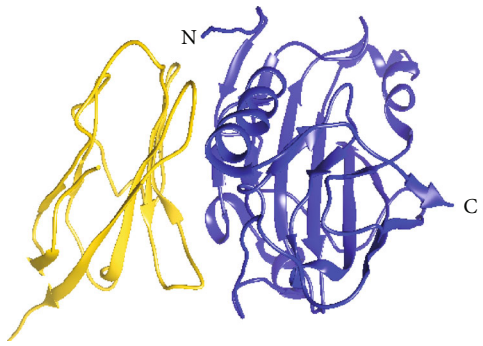

Figure 6: Structure of glycoprotein D receptor complex. A ribbon diagram illustrating the atomic structure of human HHS-1 gD (blue) in complex with the human nectin-1 cell surface receptor (yellow) [25]. The binding site incorporates portions of the N-terminal peptide and the large C-terminal helix. Note the C-terminus of HHS-1 gD at the far right, opposite the recognition surface site. The figure was created from the atomic coordinate file PDB: 3SKU [9] and the program Chimera.

of the characteristic 6 cysteine positions required for disulfide bond formation. HVS gD is slightly larger than HHS-1 gD and contains additional sequence insertions at several positions, notably 48-52, 119-124, and 329-336. Both proteins have a glycosylation site predicted at a structurally equivalent Asn (HVS Asn(133) and HHS-1 Asn(119)).

In keeping with the required structural elements essential for receptor binding revealed by the HHS-1 gD nectin-1

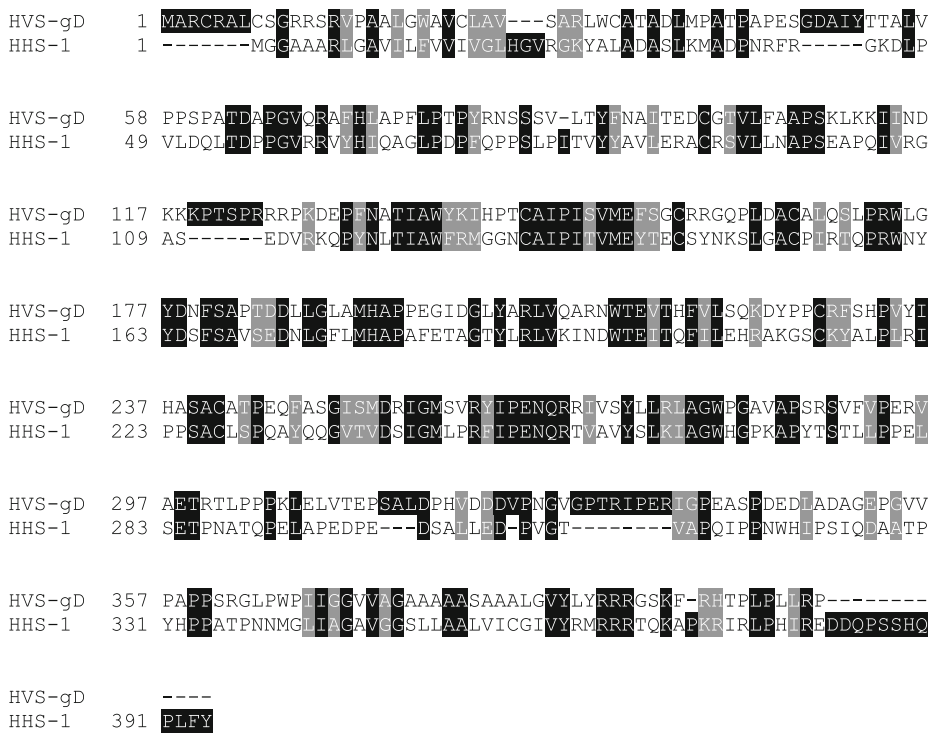

Figure 7: Sequence alignment of HVS gD and HHS-1 gD. Aligned protein sequences of HVS gD (UniProt E2IUH8) with HHS-1 gD (UniProt Q991M3). Darkly shaded areas denote conserved residues and insertions; gray shaded areas denote homologous sequence. The sequence alignment was performed with BLAST (Altschul et al., NCBI) and drawn with BOXSHADE (Hofmann and Baron).

gD_NSP for Pc_DNA3.1(+) eukaryotic expression

MARCRALCSGRRSRVPAALGWAVCLAVSARLWCATADLMPATPAPESGDAIYTTALVPP
SPATDAPGVQRAFHLAPFLPTPYRNSSSVLTYFNAITEDCGTVLFAAPSKLKKIINDKKKP
TSPRRRPKDEPFNATIAWYKIHPTCAIPISVMEFSGCRRGQPLDACALQSLPRWLGYDNF
SAPTDDLLGLAMHAPPEGIDGLYARLVQARNWTEVTHFVLSQKDYPPCRFSHPVYIHAS
ACATPEQFASGISMDRIGMSVRYIPENQRRIVSYLLRLAGWPGAVAPSRSVFVPERVAET
RTLPPPKLELVTSGGSGGSPANSTVLSFCAFAVDPAKAYKDYLASGGQPITNCVKMLCTH
TGTGQAITVTPEANMDQESFGGASCCLYCRCHIDHPNPKGFCDLKGKYVQIPTTCANDP
VGFTLRNTVCTVCGMWKGYGCS

(a)

gD_NSP for PET17b prokaryotic expression

SARLWCATADLMPATPAPESGDAIYTTALVPPSPATDAPGVQRAFHLAPFLPTPYRNSSSV
LTYFNAITEDCGTVLFAAPSKLKKIINDKKKPTSPRRRPKDEPFNATIAWYKIHPTCAIPISV
MEFSGCRRGQPLDACALQSLPRWLGYDNFSAPTDDLLGLAMHAPPEGIDGLYARLVQA
RNWTEVTHFVLSQKDYPPCRFSHPVYIHASACATPEQFASGISMDRIGMSVRYIPENQR
RIVSYLLRLAGWPGAVAPSRSVFVPERVAETRTLPPPKLELVTSGGSGGSPANSTVLSFCAF
AVDPAKAYKDYLASGGQPITNCVKMLCTHTGTGQAITVTPEANMDQESFGGASCCLYC
RCHIDHPNPKGFCDLKGKYVQIPTTCANDPVGFTLRNTVCTVCGMWKGYGCS
SGGSGGHHHHHH

(b)

Figure 8: Engineered gD-NSP (where NSP denotes the NSP10 sequence 9-129) fusion protein sequences. (a) NSP10 sequence as incorporated in pcDNA3.1 vector (following DNA optimization for expression in humans). Note: the native HVS gD transcription leader sequence is retained and there are no His-tags in this design. (b) NSP10 final sequence for incorporation in pET17b for expression in bacteria (following DNA optimization for expression in *E. coli*). Note: the viral transcription leader sequence, irrelevant in a prokaryotic expression system, has been removed and a C-terminal His-tag added. Red highlighted sequences denote linker and His-tag sequences.

complex [25], an engineered and truncated ectodomain of the HVS gD protein was then established by the examination of the crystal structure together with the aligned glycoprotein D sequences (Figure 7). Since the N-terminus and the large C-terminal helix are important components of the receptor interaction, the fusion to the NSP10 nanoparticle presentation system was accomplished through the HVS gD C-terminal section of extended polypeptide remote from the receptor binding surface, depicted in Figure 6.

The bioengineered NSP10 fusion protein was then created by appending the truncated sequence of HVS gD (residues 1-312) linked through the N-terminus of NSP10 (with the essential capsid residues 9-129, denoted NSP) with the addition of a polypeptide linker (GGSGGS) to provide greater folding flexibility and reduce potential steric interference of oligomer formation at the 3-fold axes. In the case of the prokaryotic expression using the plasmid pET17b, the N-terminal viral expression leader (residues 1-27) of HVS gD was deleted and a C-terminal His-tag sequence (SGGSGGHHHHHH) was added. The resulting amino acid sequences of the engineered NSP10 fusion proteins used for the two expression vectors are shown in Figure 8.

3.2. Eukaryotic Expression Vector and DNA Plasmid Production. The gene gD-NSP was ligated into the

expressions vector pcDNA3.1(+) using the restriction sites KpnI and XhoI (5′ and 3′, respectively). The gD-NSP gene was codon optimized for expression in humans and introduced into the expression vector such that the requirements for Kozak's sequence necessary for initiation of translation are satisfied. The resulting gD-NSP_pcDNA3.1(+) plasmid encodes for a single protein which assembles into a nanoparticle displaying an engineered truncated version of HVS gD (strain MV-5-4-PSL) (Figure 8(a)). The native viral expression leader for HVS gD was retained, and no affinity tags were incorporated into the design. Cloning, plasmid production, and quality analysis of the resulting plasmid gD-NSP_pcDNA3.1(+) including sequence verification were performed by GenScript (Canton, MA). The final sterile and endotoxin-free plasmid was formulated in PBS (0.5 mg/ml) and stored as 1 ml aliquots at -20°C.

3.3. Prokaryotic Expression Vector and Protein Purification. The gD-NSP gene shown in Figure 8(b) incorporating the addition of C-terminal His-tag residues SGGSGGHHHHHH was cloned into the bacterial expression vector pET17b using the restriction sites Nde1 and Xhol (5′ and 3′, respectively). Cloning, sequence verification, and quality analysis of the resulting plasmid gD-NSP_pET17A were performed by GenScript (Canton, MA).

Vmax™ Express chemically competent cells (SGI-DNA Inc., La Jolla, CA), a high growth rate marine gram negative, nonpathogenic bacteria *Vibrio natriegens*, were transformed and screened for Carbenicillin resistance using the manufacturer's protocol. A strain was selected with clear overexpression of a protein having the correct MW as identified by SDS-PAGE. Cells were propagated in Magicmedia™ (Thermo Fisher) at ultimately a 1-liter scale overnight, harvested by centrifugation at 8500 g and stored at -20°C. Approximately 25% of the frozen cells were brought to room temperature and lysed in Xtractor™ lysis buffer (Takara Bio USA, Mountain View, CA) for 30 minutes at room temperature with gentle shaking on an orbital shaker followed by sonication for 15 seconds. Immobilized metal affinity chromatography was used to isolate the protein (Marvelgent, Canton, MA; Cat. No. 11-0228-010). Lysed cells were centrifuged to clarification, and the supernatant added directly to the affinity media and allowed to incubate with mild mixing on an orbital shaker for 30 minutes at room temperature. The supernatant and affinity media were then centrifuged at 600 g to remove any remaining cellular debris and resuspended repeatedly using the same procedure to clarify the media before placing in the chromatography column. The packed bed (approximately 5 ml in bed volume) was further rinsed with 10 column volumes of 50 mM Tris pH 7.5 300 mM NaCl buffer. The target protein was eluted with 250 mM imidazole in the same buffer to yield approximately 7 mg of product. The total yield of His-tag-purified product from 1-liter culture was ~28 mg. The eluted protein was concentrated and buffer exchanged using 100 K MW cutoff centrifugal filter units (Amicon Ultra Cat. No. UFC910096, regenerated cellulose) to remove the imidazole and lower MW protein contaminants. The protein solubility and stability characteristics were also examined in both Tris and PBS buffers and further purified by high MW dialysis membrane 300,000 cutoff (Spectra/Por™ Cat. No. G23507) for periods of 48 hours without significant loss of material. The final purified protein was buffer exchanged into PBS containing 10% glycerol, concentrated to 1.4 mg/ml as determined by Bradford Analysis, 0.2 *u*M sterile filtered (Nalgene Syringe Filter, 25 mm, surfactant-free cellulose acetate membrane, Cat. No. 723-2520), and stored at -80°C in 1 ml aliquots.

3.4. Gel Electrophoresis. The gD-NSP from the prokaryotic expression was evaluated using both SDS-PAGE (4-20% gels; GenScript Cat No. M42010) and Native PAGE following manufactures protocols (NativePAGE™ 3-12% Bis-Tris Gels: Invitrogen/Thermo Fisher Scientific, Cat No. BN1001). Ferritin from equine spleen (Sigma-Aldrich, Cat No. F4503) and hen's egg ovalbumin (Sigma-Aldrich, Cat No. A5503) were used as comparative MW standards.

3.5. Transmission Electron Microscopy (TEM). Diluted samples of purified gD-NSP were applied to formvar-coated copper grids and negatively stained with 0.7% uranyl formate. Images were taken at 150,000x with an FEI (now Thermo Fisher) Tecnai T-12 transmission electron microscope.

3.6. Animal Studies. Animal studies were conducted separately for the two forms of vaccine in individual rabbits (two total). DNA injections of gD-NSP_pcDNA3.1+ were comprised of three 500 μg IP (500 μg/ml in PBS) injections on days 0, 21, and 63 with serum draws on days 0, 21, 42, 63, and 84. Protein injections were comprised of three IM injections (1 mg and 0.1 mg, 0.2 mg) prepared with the adjuvant Adavax™ (InvivoGen, San Diego, CA) according to manufacturer's instructions. Injections were at Days 0, 21, and 63 with serum draws on days 0, 21, 42, 63, and 84. Both the DNA and protein formulations were sterile. The animal experiments and ELISA tests were performed under contract by ProSci Inc. (Alameda, CA). ProSci Inc. animal services are in ethical compliance with NIH/OLAW and operates under USDA License.

4. Discussion and Conclusions

We have presented NSP10, a viral transcription factor found in the replicase polyprotein 1a (pp1a) of the human SARS coronavirus, as a new approach to creating self-assembling nanoparticles for a variety of fusion protein applications. NSP10 is a 17 kD gene regulatory/transcription factor thus far unique to the coronavirus family, which self-assembles to form a dodecahedron of approximately 86 Å in diameter. An overview of the vaccine design advantages of the system has been presented. Among the advantages, an extraordinary feature of this nanoparticle is the surface availability and spatial arrangement of both the N- and C-termini at each particle 3-fold symmetry axis (8 in total) with radial positions from the axes of ~8 and 10 Å, respectively. This allows nanoparticle surface displays of antigens through either terminus and is an ideal format for the fusion of trihelical stalk domains and fibrous stems which typically have radial distributions of approximately 5 Å and 8 Å, respectively.

The development of a framework for an NSP10-based approach to a vaccine for IPF has also been presented. IPF is a devastating and debilitating fatal lung disease for which a gamma herpesvirus has been strongly implicated as the etiological agent [12, 14, 28], although there is currently no clear consensus on the cause of this disease. In IPF, as with many other pathogen-based diseases, such as shingles, tuberculosis, HCMV, and Kaposi's sarcoma, the disease onset is often later in life and/or associated with a weakened immune system. We therefore postulated that a potential prophylactic or therapeutic vaccine for IPF can be used to (1) prevent IPF in individuals in the early stages of disease progression, similar to the approach used for shingles; (2) halt or slow the further development of the disease; and (3) that a vaccine used in combination with antivirals or other therapeutics may eliminate the causative induction of the aberrant immune/-repair mechanisms presumably a result of the expression of viral immune-regulatory proteins expressed during the latent phase. The viral theory of human IPF is further supported by the observations of improvements seen using antiviral therapies [16]. Currently, FDA-approved therapeutics for IPF only address factors which may improve symptoms or slow disease progression [20, 21] and many of the widely prescribed therapeutics for IPF have serious side effects which limit their effectiveness. There is currently no cure for IPF, and new approaches and treatments are urgently needed. We therefore undertook the exploration and rapid development of an NSP10-based therapeutic vaccine to target the virus HVS implicated as the etiological agent for IPF based on the scientifically compelling work of Folcik et al. [12].

In order to evaluate the design, expression, and preliminary immunological properties of NSP10 fusion proteins for this purpose, we chose gD of HVS as the initial antigenic fusion based on promising reports by others using the equivalent monomeric protein in HHS-2 vaccine development [27]. This approach was further supported after the completion of this work by the recent report of encouraging results in mice and horses using TLR-5 and gD-based DNA vaccine for Equine herpesvirus 1 (EHV-1) which causes high economic burden in the equine industry [29]. The resulting NSP10 protein gD-NSP was shown to express well in a prokaryotic expression system and purify easily with immobilized affinity chromatography. Self-assembly of gD-NSP monomer was supported by the retention in 300,000 MW cutoff dialysis membranes, electrophoretic migration observations using Native PAGE (Figure 4), and visualization of nanoparticles of the appropriate size and characteristics by TEM (Figure 5). Additionally, it is well established that nanoparticle-based antigen presentation often yields titers dramatically higher than the antigen presented in its monomeric form by tradition adjuvants alone. The preliminary examination of gD-NSP nanoparticles, as demonstrated here, also show these enhanced immunogenic properties in animals (Table 1).

Currently, the general poor immunogenicity of DNA-based vaccines has limited their broader application and a variety of approaches are being explored to overcome this limitation, including DNA prime-protein boost approaches, electroporation, and the use of novel adjuvants [30–32]. Here, we have shown that exceptional titers can be achieved using the NSP10-based DNA vaccine alone by simple injection in PBS . Considering the inherent safety and track record of pcDNA3.1 and other DNA-based vaccines, gD-NSP-pcDNA3.1 may be a viable future candidate for exploration in humans.

In addition to high immunogenicity, both the DNA and protein nanoparticles show other important vaccine advantages. We observed for the prokaryotic-expressed protein, solubility, and compatibility at physiological pH, as well as advantages in purification by high MW dialysis methods and 0.2 μM sterile filtration. In this preliminary work, the expression characteristics and physical properties of the expressed eukaryotic gD-NSP recombinant protein, including stability, were not characterized. However, the detection of significant DNA plasmid induced titers against the prokaryotic expressed protein clearly indicates that sufficient dD-NSP antigen for vaccine purposes is expressed by the pcDNA3.1+ plasmid. A more in-depth characterization of these properties including posttranslational modification will be examined in follow-up studies. While the properties of nanoparticle fusion proteins will certainly vary with the chemical nature of the fusion partners, in this case, the gD-NSP protein has been shown to be highly suitable for exploring the development of a practical therapeutic or prophylactic nanoparticle-based vaccine for HVS-implicated IPF.

Based on these initial positive results, we can now expand the study to characterize the immunology in an appropriate animal model and pursue the exploration of secondary antigens at the C-terminus, such as the HVS versions of UL40 (tegument protein VP13/14), which has been shown to be important as a T cell immunogen in HHS-2 [33]. If successful, this approach can potentially be applied to a number important herpesvirus targets causing high morbidity and mortality in immune suppressed individuals, including HCMV and Kaposi's-related sarcoma.

In summary, we report here for the first time the potential for NSP10 fusion proteins in vaccine development and provide an illustrative example of its advantages and application in the development of a first-in-class therapeutic or prophylactic vaccine for IPF. The unusual architecture and versatility of the nanoparticle provides a simplified approach for the fusion of pathogen receptor stems and other proteins or peptides without sequence polarity restrictions, making it possible for the rapid development of vaccine candidates for a broad spectrum of potential microbial and viral pathogens, including influenza virus, HIV, and tuberculosis.

Data Availability

All relevant data are within the paper.

Conflicts of Interest

DCC is the inventor and holder of a pending patent application, "NSP10 Self-Assembling Fusion Proteins for Vaccines, Therapeutics, Diagnostics and other Nanomaterial Applications," US Application No. 2018;15/768,250

concerning nanoparticle technology described herein. The remaining authors declare that no competing interests exist.

Authors' Contributions

DCC conceived and designed the experiments. DCC, BW, EW, WGJ, and JPR performed the experiment. DCC, WGJ, and BW analyzed the data. DCC with assistance from BW and EW wrote the paper.

Acknowledgments

Electron microscopy was performed in part through the use of the Vanderbilt University Cell Imaging Shared Resource Center (supported by NIH grants CA68485, DK20593, DK58404, DK59637, and EY08126).

Supplementary Materials

Table S1: ELISA optical density measurements. Animal titers from immunized rabbits #21915 and #21917 were measured by standard qualitative ELISA methods on multiwell plates coated with gD-NSP (1.4 mg/ml). The titer reported is the inverse of the reciprocal of last dilution giving an OD of equal to or greater than 0.1. The 0.1 OD positive cutoff criteria was determined empirically by calculating the mean ($m = 0.639$) and standard deviation ($s = 0.0105$) of the prebleeds ($N = 24$) combined from both animals. A threshold value for a positive titer (Pc) was calculated as $Pc \geq m + 3s = 0.095$. The values are qualitative measurements intended to guide antibody production services. The animal and antibody services, including the ELISA measurements, were performed under an animal service contract with ProSci (Alameda, CA). *(Supplementary Materials)*

References

[1] D. C. Carter and C. Li, "Genetically engineered ferritin as a vehicle for vaccine production, biomaterials, oxygen transport, and therapeutic delivery," U S Patent No. 2006;7,097,841.

[2] M. Kanekiyo, C. J. Wei, H. M. Yassine et al., "Self-assembling influenza nanoparticle vaccines elicit broadly neutralizing H1N1 antibodies," *Nature*, vol. 499, no. 7456, pp. 102–106, 2013.

[3] M. Kanekiyo, W. Bu, M. G. Joyce et al., "Rational design of an Epstein-Barr virus vaccine targeting the receptor-binding site," *Cell*, vol. 162, no. 5, pp. 1090–1100, 2015.

[4] C. Li, E. Soistman, and D. C. Carter, "Ferritin nanoparticle technology: a new platform for antigen presentation and vaccine development," *Industrial Biotechnology*, vol. 2, no. 2, pp. 143–147, 2006.

[5] Z. Wang, C. Li, M. Ellenburg et al., "Structure of human ferritin L chain," *Acta Crystallographica. Section D, Biological Crystallography*, vol. 62, no. 7, pp. 800–806, 2006.

[6] T. Tokatlian, B. J. Read, C. A. Jones et al., "Innate immune recognition of glycans targets HIV nanoparticle immunogens to germinal centers," *Science*, vol. 363, no. 6427, pp. 649–654, 2019.

[7] J. Cohen, "A Once-in-a-Lifetime Flu Shot?," *Science*, vol. 341, no. 6151, p. 1171, 2013.

[8] D. C. Carter, "NSP10 Self-Assembling Fusion Proteins for Vaccines, Therapeutics, Diagnostics and other Nanomaterial Applications," US Application No. 2018;15/768,250.

[9] D. Su, Z. Lou, F. Sun et al., "Dodecamer structure of severe acute respiratory syndrome coronavirus nonstructural protein nsp10," *Journal of Virology*, vol. 80, no. 16, pp. 7902–7908, 2006.

[10] K. Papanikolopoulou, S. Teixeira, H. Belrhali, V. T. Forsyth, A. Mitraki, and M. J. van Raaij, "Adenovirus fibre shaft sequences fold into the native triple beta-spiral fold when N-terminally fused to the bacteriophage T4 fibritin foldon trimerisation motif," *Journal of Molecular Biology*, vol. 342, no. 1, pp. 219–227, 2004.

[11] K. Papanikolopoulou, V. Forge, P. Goeltz, and A. Mitraki, "Formation of highly stable chimeric trimers by fusion of an adenovirus fiber shaft fragment with the foldon domain of bacteriophage t4 fibritin," *The Journal of Biological Chemistry*, vol. 279, no. 10, pp. 8991–8998, 2004.

[12] V. A. Folcik, M. Garofalo, J. Coleman et al., "Idiopathic pulmonary fibrosis is strongly associated with productive infection by herpesvirus saimiri," *Modern Pathology*, vol. 27, no. 6, pp. 851–862, 2014.

[13] H. Fickenscher and B. Fleckenstein, "Herpesvirus saimiri," *Philosophical Transactions of the Royal Society of London. Series B, Biological Sciences*, vol. 356, no. 1408, pp. 545–567, 2001.

[14] K. J. Williams, "Gammaherpesviruses and pulmonary fibrosis: evidence from humans, horses, and rodents," *Veterinary Pathology*, vol. 51, no. 2, pp. 372–384, 2014.

[15] G. Ma, W. Azab, and N. Osterrieder, "Equine herpesviruses type 1 (EHV-1) and 4 (EHV-4)–masters of co-evolution and a constant threat to equids and beyond," *Veterinary Microbiology*, vol. 167, no. 1-2, pp. 123–134, 2013.

[16] A. L. Mora, E. Torres-González, M. Rojas et al., "Control of virus reactivation arrests pulmonary herpesvirus-induced fibrosis in IFN-gamma receptor-deficient mice," *American Journal of Respiratory and Critical Care Medicine*, vol. 175, no. 11, pp. 1139–1150, 2007.

[17] D. J. Lederer and F. J. Martinez, "Idiopathic pulmonary fibrosis," *The New England Journal of Medicine*, vol. 378, no. 19, pp. 1811–1823, 2018.

[18] H. R. Collard, B. B. Moore, K. R. Flaherty et al., "Acute exacerbations of idiopathic pulmonary fibrosis," *American Journal of Respiratory and Critical Care Medicine*, vol. 176, no. 7, pp. 636–643, 2007.

[19] G. Raghu, H. R. Collard, J. J. Egan et al., "An official ATS/ERS/JRS/ALAT statement: idiopathic pulmonary fibrosis: evidence-based guidelines for diagnosis and management," *American Journal of Respiratory and Critical Care Medicine*, vol. 183, no. 6, pp. 788–824, 2011.

[20] T. E. King Jr., W. Z. Bradford, S. Castro-Bernardini et al., "A phase 3 trial of pirfenidone in patients with idiopathic pulmonary fibrosis," *The New England Journal of Medicine*, vol. 370, no. 22, pp. 2083–2092, 2014.

[21] L. Richeldi, R. M. du Bois, G. Raghu et al., "Efficacy and safety of nintedanib in idiopathic pulmonary fibrosis," *The New England Journal of Medicine*, vol. 370, no. 22, pp. 2071–2082, 2014.

[22] A. L. Olson, J. J. Swigris, D. C. Lezotte, J. M. Norris, C. G. Wilson, and K. K. Brown, "Mortality from pulmonary fibrosis increased in the United States from 1992 to 2003," *American Journal of Respiratory and Critical Care Medicine*, vol. 176, no. 3, pp. 277–284, 2007.

[23] M. T. Hensel, J. D. Marshall, M. R. Dorwart et al., "Prophylactic herpes simplex virus 2 (HSV-2) vaccines adjuvanted with stable emulsion and Toll-like receptor 9 agonist induce a robust HSV-2-specific cell-mediated immune response, protect against symptomatic disease, and reduce the latent viral reservoir," *Journal of Virology*, vol. 91, no. 9, 2017.

[24] D. J. Weed and A. V. Nicola, "Herpes simplex virus membrane fusion," *Advances in Anatomy, Embryology, and Cell Biology*, vol. 223, pp. 29–47, 2017.

[25] P. Di Giovine, E. C. Settembre, A. K. Bhargava et al., "Structure of herpes simplex virus glycoprotein D bound to the human receptor nectin-1," *PLoS Pathogens*, vol. 7, no. 9, 2011.

[26] T. M. Cairns, Z. Y. Huang, J. R. Gallagher et al., "Patient-specific neutralizing antibody responses to herpes simplex virus are attributed to epitopes on gD, gB, or both and can be type specific," *Journal of Virology*, vol. 89, no. 18, pp. 9213–9231, 2015.

[27] D. V. Ablashi and J. M. Easton, "Preventive vaccination against Herpesvirus saimiri-induced neoplasia," *Cancer Research*, vol. 36, pp. 701–703, 1976.

[28] Y. W. Tang, J. E. Johnson, P. J. Browning et al., "Herpesvirus DNA is consistently detected in lungs of patients with idiopathic pulmonary fibrosis," *Journal of Clinical Microbiology*, vol. 41, no. 6, pp. 2633–2640, 2003.

[29] Y. Zhao, J. Chang, B. Zhang et al., "TLR-5 agonist Salmonella abortus equi flagellin FliC enhances FliC-gD-based DNA vaccination against equine herpesvirus 1 infection," *Archives of Virology*, vol. 164, no. 5, pp. 1371–1382, 2019.

[30] L. Li, F. Saade, and N. Petrovsky, "The future of human DNA vaccines," *Journal of Biotechnology*, vol. 162, no. 2-3, pp. 171–182, 2012.

[31] L. Li and N. Petrovsky, "Molecular mechanisms for enhanced DNA vaccine immunogenicity," *Expert Review of Vaccines*, vol. 15, no. 3, pp. 313–329, 2016.

[32] L. Li and N. Petrovsky, "Molecular adjuvants for DNA vaccines," *Current Issues in Molecular Biology*, vol. 22, pp. 17–40, 2017.

[33] S. Awasthi, G. G. Mahairas, C. E. Shaw et al., "A dual-modality herpes simplex virus 2 vaccine for preventing genital herpes by using glycoprotein C and D subunit antigens to induce potent antibody responses and adenovirus vectors containing capsid and tegument proteins as T cell immunogens," *Journal of Virology*, vol. 89, no. 16, pp. 8497–8509, 2015.